OXFORD

BRIEF REPORT

Effect of Fluorinert on the Histological Properties of Formalin-Fixed Human Brain Tissue

Juan Eugenio Iglesias, PhD, Shauna Crampsie, MSc, Catherine Strand, MSc, Mohamed Tachrount, PhD, David L. Thomas, PhD, and Janice L. Holton, PhD

Abstract

Fluorinert (perfluorocarbon) represents an inexpensive option for minimizing susceptibility artifacts in ex vivo brain MRI scanning, and provides an alternative to Fomblin. However, its impact on fixed tissue and histological analysis has not been rigorously and quantitatively validated. In this study, we excised tissue blocks from 2 brain regions (frontal pole and cerebellum) of 5 formalin-fixed specimens (2 progressive supranuclear palsy cases, 3 controls). We excised 2 blocks per region per case (20 blocks in total), one of which was subsequently immersed in Fluorinert for a week and then returned to a container with formalin. The other block from each region was kept in formalin for use as control. The tissue blocks were then sectioned and histological analysis was performed on each, including routine stains and immunohistochemistry. Visual inspection of the stained histological sections by an experienced neuropathologist through the microscope did not reveal any discernible differences between any of the samples. Moreover, quantitative analysis based on automated image patch classification showed that the samples were almost indistinguishable for a state-of-the-art classifier based on a deep convolutional neural network. The results showed that Fluorinert has no effect on subsequent histological analysis of the tissue even after a long (1 week) period of immersion, which is sufficient for even the lengthiest scanning protocols.

Key Words: Ex vivo, Fluorinert, Histology, MRI.

INTRODUCTION

Ex vivo MRI is being used increasingly widely as a neuroimaging technique: since motion artifacts are not an issue, long acquisition protocols are possible (even tens of hours) to achieve ultra-high-resolution images of brain structure with high signal-to-noise ratio. To avoid susceptibility artifacts arising from tissue-air interfaces at the edges of the brain, samples may be immersed in a surrounding fluid. However, keeping the samples in the formalin fixative for this purpose is problematic due to its high proton density, which is likely to saturate the MR signal and reduce the dynamic range of the resulting images. A widespread solution to these problems is to immerse the sample in a proton-free fluid instead, which matches the magnetic susceptibility of brain tissue but has no intrinsic MR signal itself, and so is not visible in the subsequent images.

Two popular choices for proton-free fluids in ex vivo MRI scanning are Fomblin (1) (Solvay, Brussels, Belgium) and Fluorinert (2) (3 M, Maplewood, MN). Fomblin is a perfluoropolyether, which is a type of fluorocarbon-based polymer (fluoropolymer), and is most typically used as a lubricant. Fluorinert is another fluorocarbon-based fluid, which is mostly used as an electronics coolant. Both of them have high specific weight, which naturally helps to displace air inclusions at the surface of the tissue, though complete removal of all air bubbles in larger samples is difficult to achieve.

Fomblin and Fluorinert have been used in wide array of ex vivo MRI studies. For example, Miller et al used Fomblin in a diffusion-weighted imaging study of the human brain (3). Our group has previously used Fomblin in a study of the subthalamic nucleus (4). In more recent work (5), we used Fluorinert for structural scanning of whole human brain. Fomblin and Fluorinert have also been used in the scanning of brains of other species, such as mouse (6) (Fomblin) or zebra finch (7) (Fluorinert). Moreover, they have also been used to scan organs other than brain, e.g. the aorta using Fomblin (8) or the tibia using Fluorinert (9).

Despite their widespread use, the effect of these 2 fluorocarbon-based fluids on brain tissue has not been thoroughly studied. This is a critical aspect when histological analysis is performed after the MRI scanning. Some works have commented on these effects in a qualitative fashion, e.g. "Fomblin ... does not interfere with signal from various biological tissues" (10); or "High magnification examination of

the sections revealed that immersion of the tissues in Gadolinium and Fluorinert still allowed further classical histological observation of spinal cord tissues" (11). However, more rigorous analyses are necessary. To the best of our knowledge, only the effect of Fomblin on tissue has been explicitly investigated in a short conference abstract (12). This pilot study concluded that immersion in Fomblin for 48 hours had no effect on the quantitative MRI properties of mouse brain tissue; the effect on the histology was only assessed qualitatively in Figure 2 of the abstract.

General-purpose Fluorinert is significantly less expensive than MRI-grade Fomblin.[1] Therefore, general-purpose Fluorinert is a particularly attractive option for human brain scanning since large amounts of fluid (kilograms) can be required to adequately surround the specimen. However, the effect of Fluorinert on tissue has never been assessed. In this study, 10 human tissue blocks from 2 different brain regions and 5 specimens were placed in Fluorinert for a whole week, whereas neighboring blocks from the same regions and specimens remained in formalin and were never immersed in the fluorocarbon-based fluid. Subsequently, we performed a histological analysis of the samples. We then compared the stained sections to assess the impact of the exposure to Fluorinert on the histological properties of the tissue. This assessment was both qualitative (microscopy) and quantitative, showing that the discrimination of image patches from the samples that have and have not been exposed to Fluorinert is very difficult for a state-of-the-art classifier based on a deep convolutional neural network.

MATERIALS AND METHODS

In this study, we used tissue from human brains of 5 donors: 3 males and 2 females (ages of death: 61–94). Tissue was donated for research to the Queen Square Brain Bank for Neurological Disorders, UCL Institute of Neurology. The brain donation program and protocols have received ethical approval for research by the NRES Committee London—Central and tissue is stored for research under a license issued by the Human Tissue Authority (No. 12198). The postmortem intervals were between 12 and 43 hours, and the brains were received by the Queen Square Brain Bank within 96 hours after death. The brains were hemisected, the right hemispheres were frozen, and the left hemispheres were fixed in 10% neutral buffered formalin. The fixation times at sample collection ranged between 440 and 546 days.

Three brains were from neurologically normal subjects but histological examination revealed age-related tau pathology of Alzheimer type, vascular pathology in the form of small vessel disease, and atheromatous plaques in leptomeningeal vessels. Two brains were diagnosed with progressive supranuclear palsy (PSP), and also showed age-related Alzheimer disease pathology and vascular pathology in the form

---

1 In November 2016, we obtained the following two quotes: Fomblin MED 08 (designed for MRI scanning): 3000.00 EUR/kg; Fluorinert FC-3283 (general purpose), used in this study: 470 GBP for 5 kg, which was approximately equivalent to 108 EUR/kg.

of small vessel disease. The demographics of the 5 cases are summarized in Table 1.

Two neighboring blocks of tissue (thickness: 5 mm) were excised from the frontal pole and the cerebellum of the fixed left hemispheres. From each pair of blocks, one was placed in a container filled with Fluorinert FC-3283, which produces negligible MR signal; the other was immediately placed back in Formalin, playing the role of control in terms of exposure to Fluorinert. The blocks immersed in Fluorinert remained in the container for 7 days before being washed and returned to back to formalin.

All blocks were processed for paraffin wax embedding, and subsequently sectioned and stained using routine histological stains, including Hematoxylin and eosin (H&E), Luxol fast blue with Cresyl violet as a Nissl stain (LFB-Nissl), and immunohistochemistry for the following primary antibodies: myelin basic protein (MBP), clone SMI-94, mouse monoclonal, dilution 1:500, supplied by Covance (Princeton, NJ); phosphorylated neurofilament, clone SMI-31, mouse monoclonal, dilution 1:1000, supplied by Covance; phosphorylated tau, clone AT8, mouse monoclonal, dilution 1:1000, supplied by Thermo Fisher Scientific (Waltham, MA); and glial fibrillary acidic protein, clone GFAP, rabbit polyclonal, dilution 1:1000, supplied by Agilent-Dako (Santa Clara, CA).

For the immunohistochemistry, the samples were first treated in super access buffer using a pretreatment unit (A. Menarini Diagnostics, Wokingham, UK). The pretreated sections were subsequently washed in water and stained on an Menarini Intellipath automated staining machine. Finally, the stained sections were examined using a Nikon Eclipse N*i* microscope, and digitized at ×40, ×20, and ×1 magnification with an Olympus VS120 microscope/slide scanner.

For quantitative analysis, we used the experimental procedure summarized in Figure 1. First, we used an interactive segmentation method (Random Walker) (13) to extract the tissue from the background of the sections, based on manually drawn brushstrokes on the foreground and background of the images at ×1 magnification (for faster processing). The foreground masks were used to compute a min-max normalizing intensity transform for each section. Finally, 5000 patches of size 224 × 224 pixels were randomly sampled from the foreground of the sections at ×20 and ×40 magnification, and their intensities corrected with the corresponding min-max normalizing transforms. We used relatively large magnifications in the experiment as they better show whether the staining is of good quality and identifies the expected structures.

The goal of the quantitative analysis is to show that there are no significant differences between the patches of sections of tissue that have been exposed to Fluorinert compared with the controls. Comparing red-green-blue (RGB) or hue-saturation-intensity (HIS) values is not sufficient because RGB and HIS differences are effectively filtered out by the min-max histogram normalization. Instead, we used a cross validation scheme with 2-fold, in which the patches from one of the folds were used to train a state-of-the-art classifier (a deep convolutional neural network or CNN) to classify patches as exposed to Fluorinert or not, and the trained CNN was subsequently used to classify the patches of the other fold. For the CNN, we used the popular VGG-16 architecture (14)

TABLE 1. Demographics of the Cases Used in This Study

Case	Gender	Age of Death	Post Mortem Interval	Fixation Time at Sample Collection	Findings From Histological Examination
Neurologically normal	Female	84	41 hours	546 days	• Small vessel disease (mild) • Low level AD • Cerebral amyloid angiopathy (mild leptomeningeal and cortical)
Neurologically normal	Male	80	12 hours	545 days	• Small vessel disease • Atheroma • Cerebral infarct • Low level AD
Neurologically normal	Female	94	27 hours	617 days	• Small vessel disease (moderate) • Leptomeningeal vessel atheroma • Low level AD
PSP	Male	72	43 hours	469 days	• Small vessel disease • TDP-43 proteinopathy
PSP	Male	61	39 hours	440 days	• Lewy body pathology (limbic) • Small vessel disease (mild) • Argyrophilic grain disease

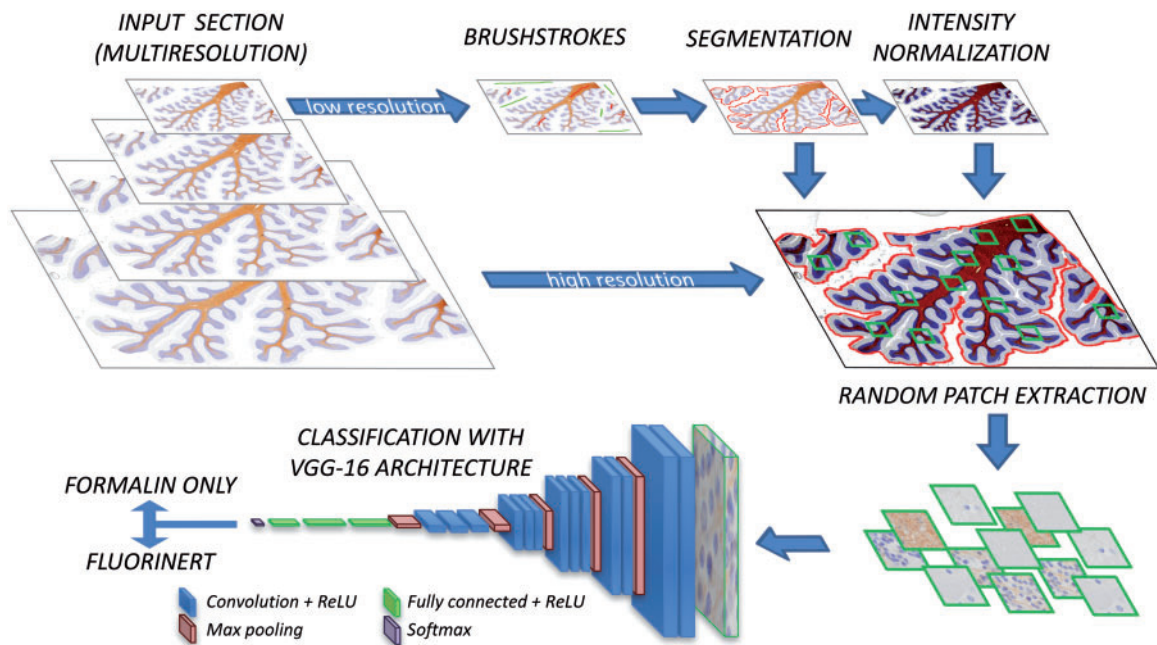AD, Alzheimer disease; PSP, progressive supranuclear palsy.

FIGURE 1. Experimental setup. The low-magnification images are interactively segmented by feeding brushstrokes to the Random Walker algorithm. The foreground mask is used to compute a min-max normalizing transform. Patches are then randomly sampled from the foreground and classified into exposed to Fluorinert vs not, by a deep convolutional neural network based on the widespread VGG-16 architecture.

pretrained on ImageNet (www.image-net.org), which includes over a million images of 1000 different categories, so the pretrained model has learned rich feature representations for a wide spectrum of images. We simply replaced the final fully connected layer of the CNN to accommodate the new number of classes (2 vs 1000). In training, we used image augmentation at the intensity (brightness/contrast) and geometric level (rotation, scaling, translation) to enrich the training dataset.

In our quantitative experiment, we recorded the accuracy to predict exposure to Fluorinert, measured at the elbow of the receiver operating characteristic curve. We also recorded the area under the curve (AUC), which provides a
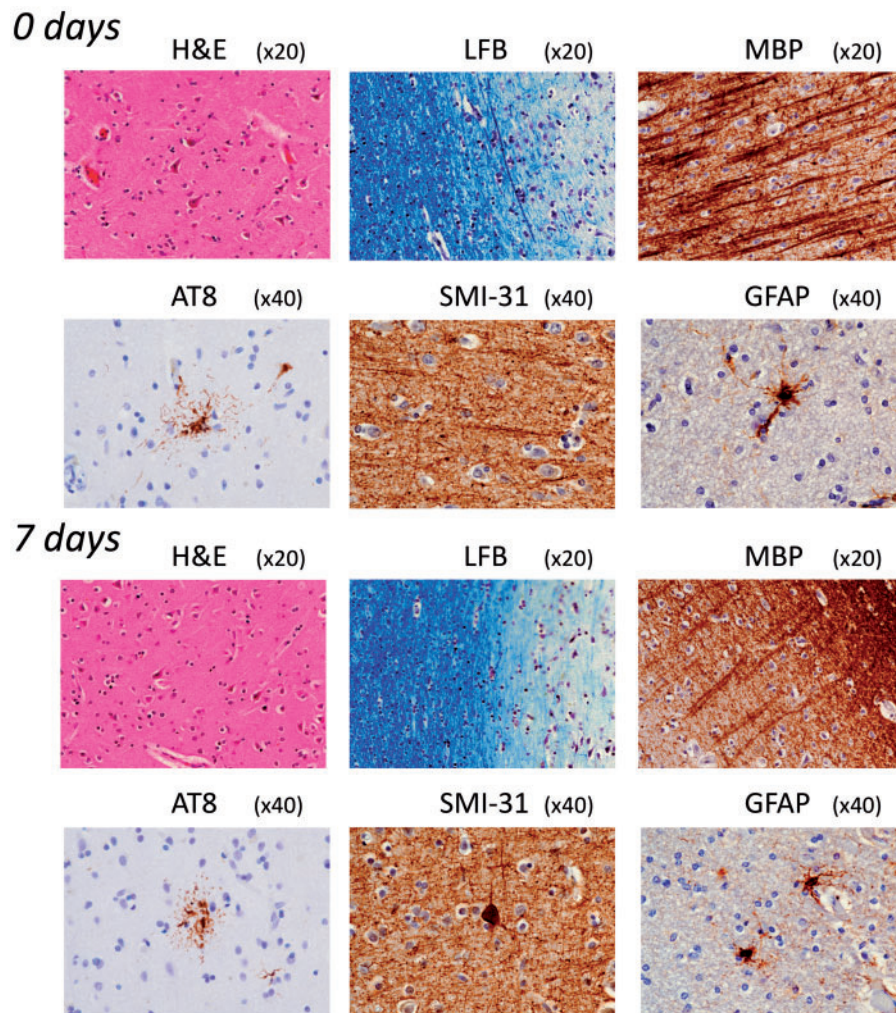
FIGURE 2. Zero vs 7-day exposure to Fluorinert in H&E and LFB-Nissl (objective ×20); and immunohistochemistry (MBP; objective ×20; AT8, SMI-31, GFAP; objective ×40). The H&E, LFB, MBP, SMI-31, and GFAP images represent a neurologically normal case. The AT8 images represent a PSP case; note that the tau inclusions are well delineated after 7 days of exposure to Fluorinert.

threshold-free measure of the discrimination ability. The same experiment was also carried out across stains, i.e. trying to predict the stain of a section from a 224 × 224 pixel patch. This experiment provides an estimate of the upper bound of the performance of the classifier.

RESULTS

Qualitative analysis of the stained sections under the microscope by an experienced neuropathologist (J.H., non-blinded) showed that, for the tissue that had been immersed in Fluorinert, the cellular integrity had not been affected, as determined using H&E to assess tissue structure and cellular morphology, supplemented by LFB-Nissl to assess myelin staining and neuronal morphology and immunohistochemical staining for MBP. Figure 2 shows examples of histological staining from the frontal pole in neurologically normal and PSP tissue that remained 0 and 7 days in Fluorinert before tissue processing, sectioning and staining. There is no substantial

difference in the morphology or staining quality in tissue immersed in Fluorinert for 7 days compared with the control tissue that had not been exposed to Fluorinert.

Immunohistochemical staining using primary antibodies for tau (AT8), phosphorylated neurofilaments (SMI-31), and astrocytes (GFAP) show comparable staining quality and intensity in all of the samples immersed in Fluorinert compared with controls (Fig. 2). Staining for tau reveals neurofibrillary tangles and threads compatible with age-related pathology in the neurologically normal cases. Importantly, in PSP cases, the diagnostic tau lesions are identified despite the immersion in Fluorinert for 7 days (see AT8 images in Fig. 2). No differences are observed in the axons with SMI-31 or in the astrocyte morphology and distribution (predominantly surrounding blood vessels) demonstrated using GFAP immunohistochemistry after 1 week of immersion in Fluorinert.

Finally, the quantitative analysis (Table 2) showed that the CNN could only make predictions marginally over chance level (i.e. 50% accuracy, AUC = 0.5), at both ×20 and ×40

TABLE 2. Accuracy at Elbow and Area Under the Curve (AUC) for Classification of Image Patches From Day 0 vs Day 7 Using a Deep Convolutional Network Based on the Widespread VGG-16 Architecture

Stain/Antibody and Objective Lens	Acc. Day 0 vs 7 (Same Stain)	AUC Day 0 vs 7 (Same Stain)	Average Accuracy vs Other Stains	Average AUC vs Other Stains
H&E ×20	55.12%	0.569	99.84% (±0.06%)	1.000 (±0.000)
LFB ×20	65.50%	0.674	98.44% (±1.58%)	0.998 (±0.002)
MBP ×20	50.09%	0.451	90.83% (±9.81%)	0.949 (±0.073)
AT8 ×20	50.06%	0.410	91.74% (±10.05%)	0.953 (±0.048)
SMI-31 ×20	50.38%	0.453	94.98% (±6.63%)	0.974 (±0.047)
GFAP ×20	51.84%	0.500	92.21% (±7.09%)	0.954 (±0.047)
H&E ×40	52.72%	0.496	99.59% (±0.06%)	1.000 (±0.000)
LFB ×40	59.85%	0.605	96.57% (±3.15%)	0.994 (±0.009)
MBP ×40	50.17%	0.432	90.50% (±9.43%)	0.943 (±0.077)
AT8 ×40	50.10%	0.443	90.14% (±9.51%)	0.940 (±0.076)
SMI-31 ×40	50.00%	0.429	94.24% (±7.77%)	0.971 (±0.053)
GFAP ×40	56.28%	0.558	90.51% (±8.08%)	0.940 (±0.056)

The average classification accuracy and AUC across other stains (at the same magnification level) are given as a reference.

magnification. This is in contrast with the discrimination of sections with different stains in which classification was close to perfect (i.e. 100% accuracy, AUC = 1.0) in most cases, due to the very different appearance of the images. The difficulties found by the classifier to separate the image patches that have been exposed to Fluorinert confirms that there is no substantial difference in the morphology or staining quality.

We note that the accuracy of the Fluorinert/control discrimination was slightly higher (∼65%) for LFB. This result can be explained by the fact that, during the staining process, the differentiation step in the LFB protocol requires that sections are processed individually by hand (as opposed to the other stains), which can result in minor differences between stained sections even though such differences are not appreciable on microscopy.

DISCUSSON

The qualitative and quantitative results presented in this paper support the hypothesis that exposure to general-purpose Fluorinert for up to a week does not have any detrimental effects on histological analysis of human brain tissue using common histological stains and a range of antibodies for immunohistological study. Visual inspection by an experienced neuropathologist did not reveal differences in cellular integrity or staining quality, and image patches from samples exposed to Fluorinert and controls were almost indistinguishable for a state-of-the-art image classifier. The findings suggest that any small effects that could have been observed would be even smaller in studies in which larger brain tissue samples are immersed, rather than the 5-mm-thick blocks used in this study, as it would be much more difficult for the Fluorinert to permeate throughout a larger sample. Therefore, we propose that Fluorinert is an inexpensive, valid option for ex vivo human brain MRI scanning and can accommodate the longest ex vivo scanning times reported in the literature (days).

While this brief report used 120 sections digitized at ×20 and ×40 magnification, covering 5 cases (including a neurodegenerative disease), 6 different stains, and 2 different brain regions, additional thorough experiments will be required to explore other interactions between Fluorinert and tissue. For instance, the range of fixation times in this study has only partly addressed the potential connection between exposure to Fluorinert, fixation time and staining quality, which may exist due to the well-known correlation between immunohistochemical staining quality and formalin fixation (15). In a similar manner, we did not explicitly test any influence of postmortem interval, which affects tissue integrity. Investigating these questions, along with testing other less common markers that may be more sensitive to Fluorinert, remains as future work.

REFERENCES

1. Simmons JH. Production of fluorocarbons I. The generalized procedure and its use with nitrogen compounds. J Electrochem Soc 1949;95:47–52
2. Caporiccio G, Flabbi L, Marchionni G, et al. The properties and applications of perfluoropolyether lubricants. J Synth Lubr 1989;6:133–49
3. Miller KL, Stagg CJ, Douaud G, et al. Diffusion imaging of whole, postmortem human brains on a clinical MRI scanner. Neuroimage 2011;57:167–81
4. Massey L, Miranda M, Zrinzo L, et al. High resolution MR anatomy of the subthalamic nucleus: Imaging at 9.4 T with histological validation. Neuroimage 2012;59:2035–44
5. Iglesias JE, Insausti R, Lerma-Usabiaga G, et al. A probabilistic atlas of the human thalamic nuclei combining ex vivo MRI and histology. Neuroimage 2018;183:314–26
6. Benveniste H, Kim K, Zhang L, et al. Magnetic resonance microscopy of the C57BL mouse brain. Neuroimage 2000;11:601–11
7. Poirier C, Vellema M, Verhoye M, et al. A three-dimensional MRI atlas of the zebra finch brain in stereotaxic coordinates. Neuroimage 2008;41:1–6
8. Lipinski MJ, Amirbekian V, Frias JC, et al. MRI to detect atherosclerosis with gadolinium-containing immunomicelles targeting the macrophage scavenger receptor. Magn Reson Med 2006;56:601–10.
9. Luhach I, Idiyatullin D, Lynch CC, et al. Rapid ex vivo imaging of PAIII prostate to bone tumor with SWIFT-MRI. Magn Reson Med 2014;72:858–63.

10. Itskovich VV, Choudhury RP, Aguinaldo JGS, et al. Characterization of aortic root atherosclerosis in ApoE knockout mice: High-resolution in vivo and ex vivo MRM with histological correlation. Magn Reson Med 2003;49:381–5

11. Noristani HN, Lonjon N, Cardoso M, et al. Correlation of in vivo and ex vivo 1H-MRI with histology in two severities of mouse spinal cord injury. Front Neuroanat 2015;9:24

12. Hyare H, Powell C, Thornton J, et al. Perfluoropolyethers in magnetic resonance microscopy: Effect on quantitative magnetic resonance imaging measures and histological properties of formalin-fixed brain tissue. Proc Int Soc Mag Res Med 2008;1719

13. Grady L. Random walks for image segmentation. IEEE Trans Pattern Anal Mach Intell 2006;28:1768–83

14. Simonyan K, Zisserman A. Very deep convolutional networks for large-scale image recognition. arXiv preprint arXiv 2014;14091556

15. Lyck L, Dalmau I, Chemnitz J, et al. Immunohistochemical markers for quantitative studies of neurons and glia in human neocortex. J Histochem Cytochem 2008;56:201–21